



A new model for the determination of optimum fiber volume fraction under multi-axial loading in polymeric composites

Fathollah Taheri-Behrooz¹ · Mahmood Mehrdad Shokrieh¹ · Hamidreza Sokhanvar¹

Received: 24 July 2018 / Accepted: 26 November 2018 / Published online: 30 November 2018
© Iran Polymer and Petrochemical Institute 2018

Abstract

Mechanical properties of composite materials are a function of fiber volume fraction. Based on the existing micromechanical models, the in-plane shear strength of these materials is decreased as their fiber volume fraction is increased. However, their compressive strength is initially increased and then it is dropped as the fiber content increases. The fiber content in the composite of maximum compressive strength was referred to as the optimum fiber volume fraction. Experiments performed in this study revealed that in-plane shear strength variation versus fiber volume fraction was to some extent similar to that of compressive strength. Moreover, different optimum fiber volume fractions for in-plane shear strength and compressive strength were observed. Consideration of both in-plane shear strength and the compressive strength in combined loading was proposed to find the optimum fiber volume fraction. The modified Hashin failure criterion by Lessard was employed to relate the longitudinal and transverse compressive stress and strength to in-plane shear stress and strength. A safe region predicted by this failure criterion was represented by plotting longitudinal compressive and in-plane shear stress relation for different fiber contents. The fiber content corresponding to the maximum safe region was introduced as the optimum fiber volume fraction. Axial compressive and in-plane shear tests were conducted for obtaining the variation of longitudinal compressive and in-plane shear strengths with fiber volume fraction. To identify the capability of the model for multi-axial state of stress, a unidirectional off-axis test was also performed. The test results on the unidirectional and off-axis composite specimens confirmed the predictions by the theoretical model.

Keywords Fiber volume fraction · Composites · Micromechanics · Compression · In-plane shear

Introduction

Composite materials because of their high strength and low weight are widely used in various industries. Considering the dependence of their strength on fiber volume fraction, determination of this parameter is critical in the design process.

Fiber volume fraction has a remarkable effect on mechanical properties of composites. The main goal of this study is to determine the optimum fiber volume fraction in which the maximum strength can be obtained. Based on the knowledge of the authors of this article, there is no report in the

literature concerning the optimum fiber volume fraction for the continuous fiber composites.

In the past 30 years, micromechanical studies presented equations for predicting the strength of composite materials [1]. Chamis [2] demonstrated a group of categorized micromechanical equations for predicting the tensile, compressive, shear and bending strengths of composite materials. A model for predicting the mode of transverse tensile failure due to Poisson's strains is presented by Agarwal et al. [3]. Karayaka et al. [4] investigated the effect of fiber volume fraction and misalignment of fibers, and the strength of matrix on the longitudinal compressive strength. It was indicated that temperature has a remarkable influence on the compressive strength failure. The experimental results revealed that two modes of failure occur at different temperatures, i.e. the transverse shear failure at 100 °C and wrinkling failure at above 100 °C which is likely due to the strength loss for the matrix by increasing the temperature. They performed a tensorial analysis to study the variation of

✉ Mahmood Mehrdad Shokrieh
Shokrieh@iust.ac.ir

¹ Composites Research Laboratory, Center of Excellence in Experimental Solid Mechanics and Dynamics, School of Mechanical Engineering, Iran University of Science and Technology, Tehran 16846-13114, Iran

mean and local field stresses as a function of misalignment of fibers, mismatch of the stiffness of the fiber and resin, and fiber volume fraction.

Haberle et al. [5] have presented an analytical micromechanical method to predict the longitudinal compressive strength of unidirectional reinforced plastics. Misalignment of the fibers and non-linear behavior of shear stress are considered in their model. Fiber alignment has been shown to be a focal factor in evaluating the compressive strength which cannot be excluded. It was inferred that the experimental results were in good agreement with carbon/epoxy composites. Another analytical micromechanical method was reported by Xu et al. [6] to predict the longitudinal compressive strength of composite materials based on the elasticity solution of a beam on an elastic foundation. The dominant mode of failure considered in their research was the micro-buckling of fibers. In their research, an equation for predicting lower longitudinal compressive strength for composites was developed. It was shown that the compressive strength profiles for T300/5208, AS/3501-6, HT-S/epoxy and E-glass fiber/epoxy vary almost linearly with fiber volume fraction.

De Moraes et al. [7] presented a numerical micromechanical model for predicting the longitudinal compressive strength. In their model, it is assumed that failure occurs in micro-buckling of fibers. Model predictions were compared with experimental data and proved in good agreement with them. Naik et al. [8] reviewed models to predict the compressive strength of unidirectional composites based on kinking and micro-buckling of fibers. They concluded that both Xu–Reifsnider and Budiansky models predict the compressive strength quite accurately while Rosen model overpredicts the strength.

Jasso et al. [9] presented a model to investigate the effect of spatial distributions in fiber volume fraction on the failure initiation location. In another work, Yoo et al. [10] indicated that at low-fiber-volume fractions ($K_f \leq 1.0\%$), the twisted fibers provided the highest flexural strength. However, they demonstrated that similar strength and lower toughness were comparable with straight fibers at K_f equal to or higher than 1.5%. Abdullah et al. [11] performed the experiment with three formulations of fiber volume fractions, namely 0% (neat), 15% and 45%. The results showed that tensile properties such as tensile strength and modulus of elasticity improved as fiber volume fraction increased. It has been shown by many researchers that adding specific percentage of nanofiber volume fraction could effectively change the mechanical and physical properties of the nanocomposites [12, 13].

The objective of this study is to determine the optimum fiber volume fraction to obtain superior mechanical properties for composite materials. To achieve this goal, the strength properties which fluctuate by increasing fiber volume fraction are considered.

Among various behaviors, the longitudinal compressive strength estimated by the failure model of Agarwal et al. [3] has an absolute maximum value. Therefore, this property is a prospective candidate to determine the optimum fiber volume fraction. Based on the above-mentioned micromechanical models, the in-plane shear strength of a unidirectional ply decreases by increasing its fiber volume fraction. However, their compressive strength first improves and then drops as the fiber content increases. For this reason, to this end, only compressive tests are used to find optimum fiber volume fraction of unidirectional composites. Consideration of both in-plane shear strength and the compressive strength in combined loading is proposed in the current research to find the optimum fiber volume fraction. The modified Hashin failure criterion by Lessard et al. [14] is employed to relate longitudinal and transverse compressive stress and strength to in-plane shear stress and strength.

As a result, the optimum fiber volume fraction in a composite layer would be obtained by considering general in-plane loading conditions.

A model for determination of optimum fiber volume fraction

Schematic behavior of the longitudinal compressive strength and in-plane shear strength of a unidirectional composite laminate versus fiber content is illustrated in Fig. 1. As shown in this figure, the optimum fiber volume fraction for these two properties is different. Therefore, to determine the optimum fiber volume fraction, a model is required to combine these results employing a suitable failure criterion. In Fig. 1, S_{mC} and S_{mS} are the compressive and shear strength of the neat resin, respectively.

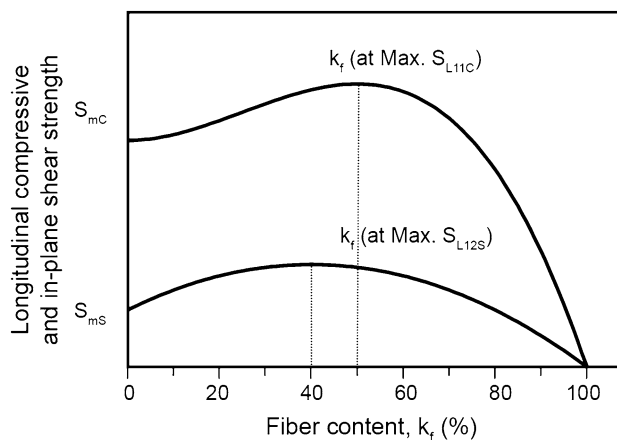


Fig. 1 Schematic behavior of longitudinal compressive and in-plane shear strengths versus fiber content

There are different failure criteria for damage prediction in composite materials [15]. The modified Hashin failure criterion by Lessard et al. [14] is employed in this study. This criterion considers six different equations to predict the different failure modes of a composite layer subjected to complete three-dimensional stress states.

For predicting the modes of failure in fiber and matrix directions subjected to compressive axial loading, the corresponding equations are as follows:

$$\left(\frac{\sigma_{L11C}}{S_{L11C}}\right)^2 + \left(\frac{\sigma_{L12S}}{S_{L12S}}\right)^2 = 1, \tag{1}$$

$$\left(\frac{\sigma_{L22C}}{S_{L22C}}\right)^2 + \left(\frac{\sigma_{L12S}}{S_{L12S}}\right)^2 = 1, \tag{2}$$

where σ_{L11C} and S_{L11C} are longitudinal compressive stress and strength, σ_{L12S} and S_{L12S} are in-plane shear stress and strength, and σ_{L22C} and S_{L22C} are transverse compressive stress and strength, respectively.

In Eq. (1), the denominator shows the strength of a unidirectional laminate as a function of fiber content (k_f) and numerator shows the stress state in the given ply.

In this study, two experimental equations were developed to predict the compressive and in-plane shear strengths of a unidirectional ply as a function of fiber content.

Substituting the compressive and in-plane shear strength equations in Eq. (1) and solving the equation for compressive and in-plane shear stress, Eq. (1) represents a quarter of ellipse as a failure space. In the graphical representation of Eq. (1), predictions of the safe region are obtained using MATLAB software shown in Fig. 2. Upon close observation, as the fiber content increases, the safe region, predicted by the failure criteria (Eq. 1), increases and then decreases. The fiber content, at maximum safe region, is known as the optimum fiber volume fraction. The main goal of this study is to define the optimum fiber volume fraction of a ply for general loading condition.

Comparison of the model predictions with real failure mode of composite materials

Off-axis compressive and tensile tests on orthotropic glass and carbon epoxy composites were performed by Yang [16] to verify the failure predictions by Tsai–Wu criterion. Similarly, compressive tests of off-axis glass/epoxy composites were used experimentally to verify the accuracy of the predicted failure surface by the model. These tests consider the interaction between the in-plane shear and the longitudinal compressive strengths.

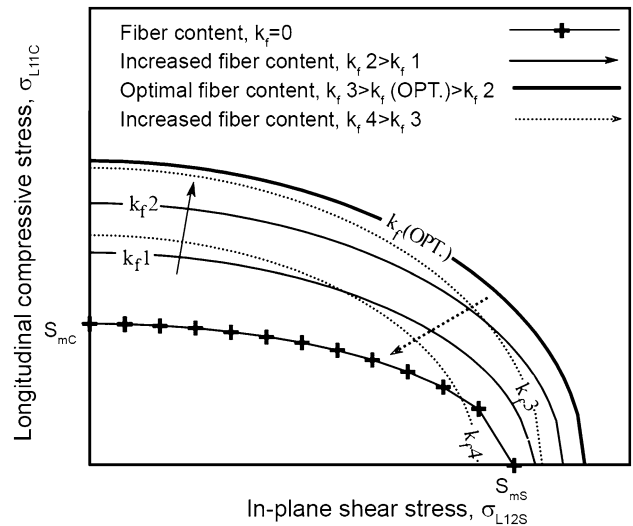


Fig. 2 A schematic presentation of the safe region predicted by Eq. (1) as a function of the fiber content

An orthotropic lamina subjected to the uniaxial normal stress, σ_x , making an angle of θ with the longitudinal direction results in biaxial stress in the composite. If one assumes $\sigma_{xy} = 0, \sigma_y = 0$, it will give

$$\begin{cases} \sigma_{L11} = \sigma_x \cos^2 \theta \\ \sigma_{L22} = \sigma_x \sin^2 \theta \\ \sigma_{L12S} = -\sigma_x \sin \theta \cos \theta. \end{cases} \tag{3}$$

One may replace the obtained on-axis stress components in Eq. (1) to predict the failure surface and obtain the off-axis strength of the unidirectional composite in compressive failure mode of the fiber as

$$S_{xf} = \left[1 - \frac{S_{L11C}^2 S_{L12S}^2}{S_{L11C}^2 \sin^2 \theta \cos^2 \theta + S_{L12S}^2 \cos^4 \theta} \right]^{\frac{1}{2}}, \tag{4}$$

where S_{xf} is the off-axis strength in the compressive failure mode of the fiber.

To compare the model predictions with the actual failure mode of composites, the off-axis specimens with fiber angle of 20° were fabricated with various fiber contents and tested under axial compressive loading in this study.

Experimental

To obtain the basic input data of the model and then verify the model predictions, three main groups of tests were carried out in this study.

The first group of tests was performed on pure resin to obtain the compressive and in-plane shear strengths and

Table 1 Mechanical properties of epoxy resin in compression and shear

	Sample 1	Sample 2	Sample 3	Sample 4	Mean
Shear strength (MPa)	63.4	63.57	64.4	–	63.79
Compressive strength (MPa)	108.5	106.6	109.3	106.4	107.77

modulus of the resin. The second group of tests was carried out to find the compressive and in-plane shear strength of the unidirectional composites at three different fiber contents. The third group of tests was performed on off-axis samples to verify the accuracy of the proposed model.

Pure resin tests

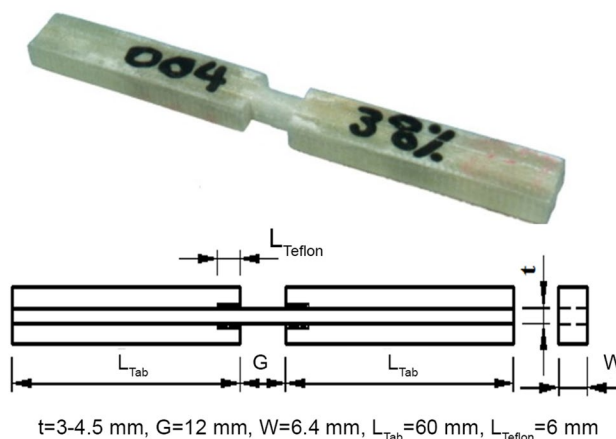
Compressive and in-plane shear tests were performed on L20 neat epoxy resin manufactured by Bakelite AG Company (Germany). Samples are manufactured according to standards ASTM D695 [17] and TQ [18], respectively. All specimens were cured at 60 °C for 16 h. In each case, four specimens were tested. The averages of test results are tabulated in Table 1. Standard deviations were 0.53 and 1.61 for compressive and in-plane shear strengths, respectively.

Testing of unidirectional on-axis specimens

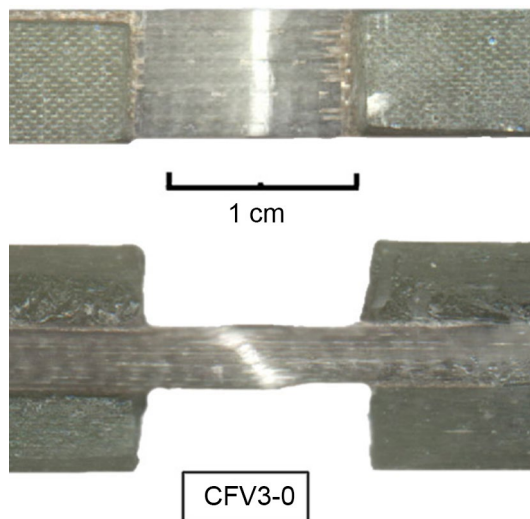
To obtain the variation of the compressive and in-plane shear strengths of the unidirectional composites with the fiber content, specimens with different fiber contents were fabricated according to ASTM D3410 [19] and ASTM D4255 [20], respectively. Compressive and in-plane shear tests of the composite specimens are carried out using 250 kN Instron universal testing machine (USA).

Unidirectional E-glass fabric with an aerial weight of 220 g/m², supplied by Inter-Glass Co., Germany, and epoxy resin L20 were used to fabricate three groups of specimens with different fiber contents. All specimens were manufactured using hand lay-up method assisted with vacuum bagging and cured for a period of 16 h at 60 °C according to the vendor instruction. The measurements of volume fraction and void content of the specimens were performed using burn out test. Tests by combined mechanical and ultrasonic methods were carried out according to the standards ASTM D2584 [21] and ASTM D5300 [22], respectively.

Figure 3 shows the fabricated compressive specimens with 38% of fiber content and its dimension. As shown in Fig. 3, to avoid premature failure of the specimens in tab area Teflon inserts were used at the end part of the tabs [23,

**Fig. 3** Fabricated compressive specimen (top) and its dimension (down)**Table 2** Axial compressive test results of glass/epoxy composites

Number of specimens	4	4	5
Standard deviation	36.697	123.241	82.161
Mean strength (MPa)	430.583	489.309	440.096
Fiber volume fraction (%)	37.94	48.07	53.29

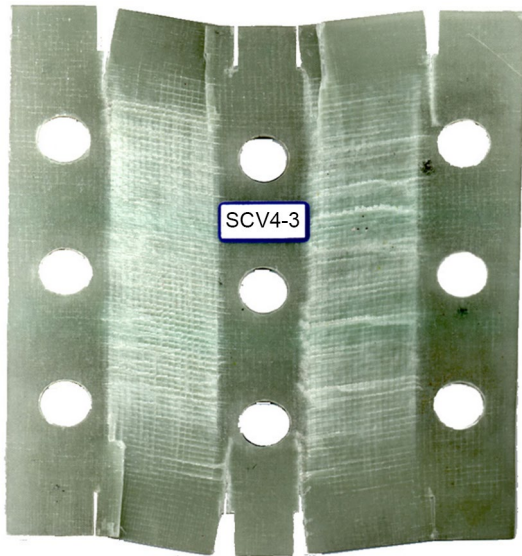
**Fig. 4** Failure mode under compressive loading

24]. Axial compressive test results are tabulated in Table 2 and the failed specimens with 53.29% of fiber content under compressive loading are shown in Fig. 4.

The in-plane shear specimens were fabricated according to the descriptions presented in Table 3 and procedure B of ASTM D4255 at fiber volume fractions of 35, 42.7 and 50.69%. As it is displayed in Fig. 5, eight notches are

Table 3 Number of plies, stacking sequence and fiber volume fraction of shear specimens

Stacking sequence	[0/90/0/90/0/90/0/90/0]	[0/90/0/90/0/90/0/90/0]	[0/90/0/90/0/90/0]
Number of plies	9	9	7
Fiber volume fraction	50.69	42.7	35

**Fig. 5** Failure mode under in-plane shear loading**Table 4** In-plane shear test results of glass/epoxy composites

Number of specimens	3	3	4
Fiber volume fraction (%)	35	42.7	50.69
Mean strength (MPa)	69.192	71.72	70.518
Standard deviation	0.711	0.8043	1.2984

added to the standard specimen to avoid stress concentration around gripping area [24]. For each case, three specimens were tested and test results are shown in Table 4. Figure 5 shows the failure mode of the in-plane shear specimen with 42.7% of fiber content.

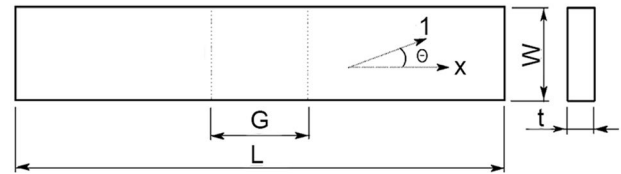
Testing of unidirectional off-axis specimens

There is no standard for the dimension of off-axis specimens. To ensure repeatability, special attention was paid to the preparation of specimens and a consistent procedure was adopted from ASTM D 3410. Unidirectional off-axis specimens were fabricated according to the specifications presented in Table 5 with the fiber angle of 20° off-axis of the fiber orientation with loading axis as shown in Fig. 6.

Specimens were fabricated with fiber volume fractions (k_f) of 39.29, 57.01 and 57.67%. These specimens were tested without end tabs. Off-axis specimens with

Table 5 Stacking sequence, length and fiber volume fraction of shear specimens

Stacking sequence	[20 ₂₇] _T	[20 ₂₉] _T	[20 ₂₀] _T
Length	25.4	25.8	25.4
Fiber volume fraction (%)	57.67	57.01	39.29

Fiber angle, $\Theta=20^\circ$, $G=25$ mm, $W=25$ mm, $t=4.5$ mm, $L=127$ mm**Fig. 6** Fabricated off-axis specimen (top) and specimen dimensions (down)**Table 6** Off-axis compression test results of glass/epoxy composites

Number of specimens	5	4	4
Fiber volume fraction (%)	39.29	57.01	57.67
Mean strength (MPa)	185.93	154.2	154.34
Standard deviation	11.15	4.5	3.5

cross-sectional dimensions of 4.5 mm by 25 mm and the length of 127 mm were produced and the average strength results along with the standard deviations are given in Table 6.

Figure 7 shows the failure mechanism in one of the off-axis specimens from top and side views.

Upon close observation, white colors in the specimen appear to be failure initiation perpendicular to the fiber direction, which indicates the failure of specimen in the shear mode. One may confirm this postulation using Eq. (4). Substituting the average off-axis strength of 185.93 MPa from Table 6 in Eq. (4), stress components in fiber, matrix, and in-plane shear directions were obtained as -164.83 , -21.75 and 58.758 , respectively. By substitution of the data

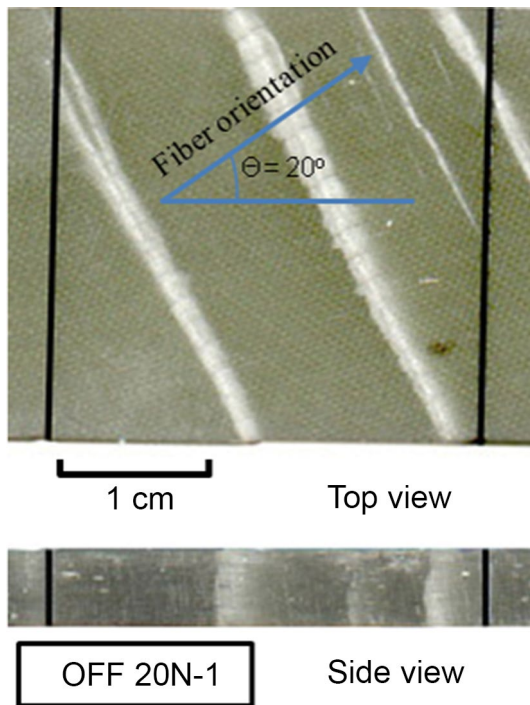


Fig. 7 Failure mode in specimen with fiber angle of 20° and fiber content of 39.29

and their relevant ultimate values in Eqs. (1) and (3) failure values of 0.89 and 0.85 were obtained for compressive fiber and compressive matrix failure modes, respectively.

Test results revealed that the mode of failure is compressive fiber breakage for these specimens. It is worthwhile to mention that predicted failure number for compressive fiber failure mode by Eq. (1) was 0.89 which was approximately 10% less than that predicted by the experiment.

Model verifications

All experiential data obtained from testing of pure resin and unidirectional composites subjected to compressive axial loading are represented in Fig. 8. A curve is fitted to the experiential data using the least square method. Due to the importance of the maximum strength, its coordinate was extracted from Fig. 8 as follows:

$$k_f = 48.7\% \Rightarrow S_{L11C} = 459.37 \text{ (MPa)}.$$

Experimental predictions are in agreement with previous studies by Xu et al. [6] for compressive tests. Furthermore, the micromechanical model introduced by Agarwal et al. [3] for compressive strength in transverse tensile failure mode predicts similar results as shown in Fig. 8.

In-plane shear test results are plotted in Fig. 9. As it is clear, the results show a smooth increase in in-plane shear

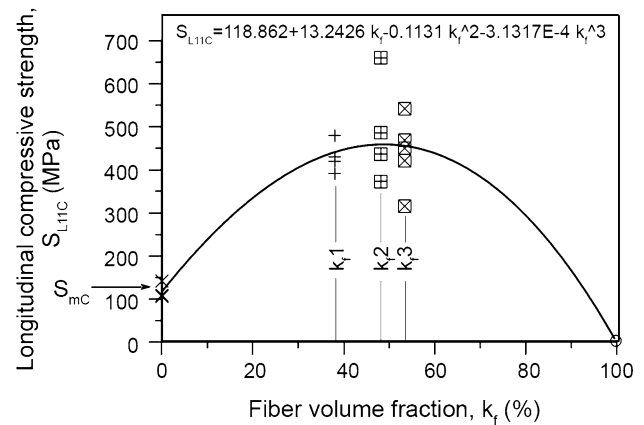


Fig. 8 Variation of compressive strength as a function of fiber content

strength value by increasing the fiber content up to a certain value and then start decreasing similar to the behavior which was seen under compressive loading (Fig. 8). This finding is not consistent with the predicted behavior by the theoretical models [1] which supports the main concept proposed in this study.

Using least square method, a curve is fitted to the experimental data and the peak value of the curve is obtained from Fig. 9 as

$$k_f = 41.08\% \Rightarrow S_{L12S} = 68.91 \text{ (MPa)}.$$

As it is expected, from Figs. 8 and 9, two different optimum fiber volume fractions were obtained as 48.7 and 41.08 under in-plane shear and compressive loading, respectively.

Two semi-empirical equations are fitted to the experimental data of Figs. 8 and 9 to represent compressive strength and in-plane shear strength of a unidirectional ply as a function of the fiber content as following:

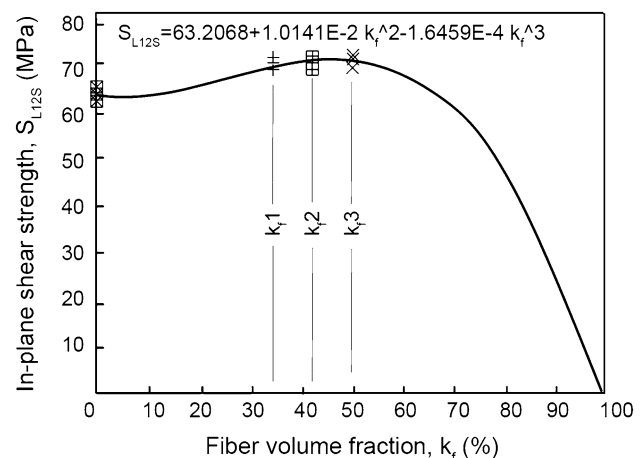


Fig. 9 In-plane shear strength of the unidirectional composite versus fiber content

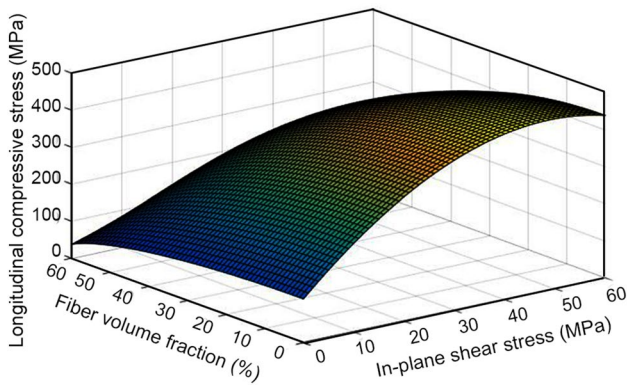


Fig. 10 3D safe region contours as a function of fiber content

$$S_{L12S} = 63.2668 + 1.0141 \times 10^{-2} k_f^2 - 1.6459 \times 10^{-4} k_f^3, \tag{5}$$

$$S_{L11C} = 118.862 + 13.2426 k_f - 0.1331 k_f^2 - 3.1317 \times 10^{-4} k_f^3. \tag{6}$$

A computer code is written to find the optimum fiber volume fraction using Eq. (1). The 3D safe region curves for different fiber contents are plotted in Fig. 10.

As depicted in Fig. 10, the optimum fiber volume fraction by the model was predicted as 46%. This optimum value lies between two predicted optimum fiber contents by the axial compression (48.7%) and in-plane shear (41.07%) of unidirectional laminates loaded in their material axis.

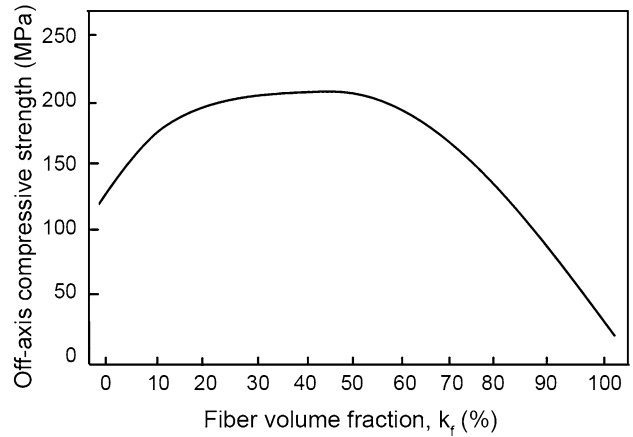
To evaluate the capability of the model in the prediction of the optimum fiber volume fraction under the multi-axial state of stress, specimens with 20° fiber angle are fabricated and tested. Test results are plotted in Fig. 11. For comparison purpose, Eq. (4) is used to predict the optimum fiber volume fraction under the multi-axial state of stress and the model prediction is shown in Fig. 11.

The optimum fiber volume fraction and the maximum compressive strength were predicted 44.6% and 176.7 MPa experimentally and 43.2% and 197.8 MPa theoretically. Error percentage appeared to be 3.2 and 10.7 for the fiber volume fraction and the compressive strength, respectively.

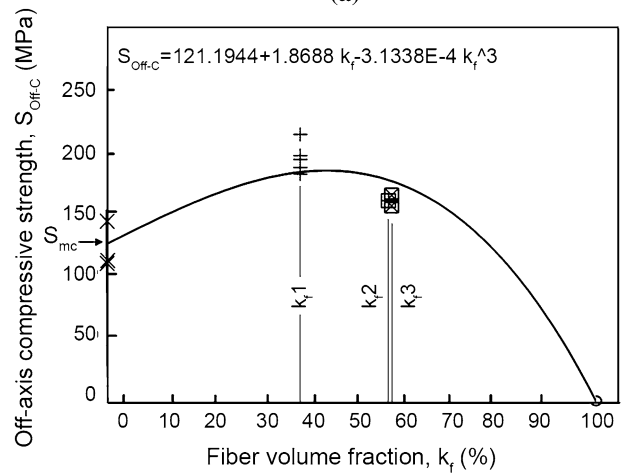
Finally, the present work demonstrated that optimum fiber volume fraction should be defined based on both compressive and in-plane shear behaviors of the composites.

Conclusion

The main goal of this study was the estimation of the optimum fiber volume fraction in fibrous composites to obtain maximum strength incorporating the effect of both longitudinal compressive strength and in-plane shear strength.



(a)



(b)

Fig. 11 Off-axis compressive strength: **a** model prediction and **b** experiment

Compressive experiments were conducted on composite specimens and compressive strength as a function of fiber content presented. Test results verified the increasing and decreasing behavior of the stress-fiber content curved as predicted by the theoretical models such as Agarwal and Broutman. In addition, the experiments were carried out on in-plane shear specimens. Results revealed an increasing and decreasing behavior for in-plane shear, which was in contradiction with predicted results suggested by theoretical models in which a decreasing behavior in the in-plane loading of the composites was only predicted.

As the predicted optimum fiber content by the compressive loading and in-plane shear loading was different, a model was introduced to address this obstacle which employed both compressive and in-plane shear properties of the composites to predict the optimum fiber content for the multi-axial state of the stress. Model prediction was eventually verified by the experiments carried on off-axis specimens and showed a good agreement.

References

1. Gibson RF (2016) Principles of composite material mechanics. CRC Press, Boca Raton
2. Chamis CC (1974) Micromechanics strength theories. Fracture and fatigue, vol 5 of composite materials. Academic Press, New York, pp 93–151
3. Agarwal BD, Broutman LJ, Chandrashekhara K (2017) Analysis and performance of fiber composites, 3rd edn. Wiley, New York
4. Karayaka M, Sehitoglu H (1996) Failure behavior of unidirectional AS4/3501-6 carbon/epoxy laminates. *J Compos Mater* 30:1150–1176
5. Haberle J, Matthews F (1994) A micromechanics model for compressive failure of unidirectional fibre-reinforced plastics. *J Compos Mater* 28:1618–1639
6. Xu YL, Reifsnider KL (1993) Micromechanical modeling of composite compressive strength. *J Compos Mater* 27:572–588
7. De Moraes AB, Marques AT (1997) A micromechanical model for the prediction of the lamina longitudinal compression strength of composite laminates. *J Compos Mater* 31:1397–1412
8. Naik N, Kumar RS (1999) Compressive strength of unidirectional composites: evaluation and comparison of prediction models. *Compos Struct* 46:299–308
9. Jasso AJM, Goodsell JE, Ritchey AJ, Pipes RB, Koslowski M (2011) A parametric study of fiber volume fraction distribution on the failure initiation location in open hole off-axis tensile specimen. *Compos Sci Technol* 71:1819–1825
10. Yoo DY, Kim S, Park GJ, Park JJ, Kim SW (2017) Effects of fiber shape, aspect ratio, and volume fraction on flexural behavior of ultra-high-performance fiber-reinforced cement composites. *Compos Struct* 174:375–388
11. Abdullah A, Khalina A, Ali A (2011) Effects of fiber volume fraction on unidirectional kenaf/epoxy composites: the transition region. *Polym Plast Technol Eng* 50:1362–1366
12. Megahed A, Megahed M (2017) Fabrication and characterization of functionally graded nanoclay/glass-fiber/epoxy hybrid nanocomposite laminates. *Iran Polym J* 26:673–680
13. Kurd SM, Hassanifard S, Hartmann S (2017) Fracture toughness of epoxy-based stepped functionally graded materials reinforced with carbon nanotubes. *Iran Polym J* 26:253–260
14. Lessard LB, Shokrieh MM (1995) Two-dimensional modeling of composite pinned-joint failure. *J Compos Mater* 29:671–697
15. Hinton M, Kaddour A (2013) Triaxial test results for fibre-reinforced composites: the second world-wide failure exercise benchmark data. *J Compos Mater* 47:653–678
16. Yang G (1994) Experimental investigation of strength criteria for S-glass, E-glass and graphite fiber composite plate. *Theor Appl Fract Mech* 20:59–66
17. ASTM (1996) Standard test method for compressive properties of rigid plastics. D695-96. American Society for Testing and Materials
18. SM21 (1982) Advanced torsion testing machine. Technical Manual, TecEquipment Ltd
19. ASTM (1995) Standard test method for compressive properties of polymer matrix composite materials with unsupported gage section by shear loading. D3410-95. American Society for Testing and Materials
20. ASTM (1983) Standard guide for testing in-plane shear properties of composite laminates. D4255-83. American Society for Testing and Materials
21. ASTM (1985) Standard test method for ignition loss of cured reinforced resins. D2584-68. American Society for Testing and Materials
22. ASTM (1993) Standard test method for measurement of resin content and other related properties of polymer matrix thermoset prepreg by combined mechanical and ultrasonic methods. D5300-93. American Society for Testing and Materials
23. Mobasher B (2016) Textile fiber composites: testing and mechanical behavior. Textile fibre composites in civil engineering. Elsevier, Dordrecht
24. Mortell D, Tanner D, McCarthy C (2017) A virtual experimental approach to microscale composites testing. *Compos Struct* 171:1–9